

TiCu₂Se₂: A p-TYPE METAL WITH A LAYER STRUCTURE

R. BERGER* and C. F. VAN BRUGGEN

Laboratory of Inorganic Chemistry, Materials Science Centre of the University, Nijenborgh 16, 9747 AG Groningen (The Netherlands)

(Received September 2, 1983)

Summary

The ternary compound TiCu₂Se₂, which has a ThCr₂Si₂-type structure, was characterized by means of miscellaneous physical measurements. It is a p-type metal with a Fermi energy of 1.3 eV. There is one hole (effective mass, 1.3 m_0) per formula unit in the valence band. In addition to metallic conduction the delocalized holes give rise to Pauli paramagnetism. There was no conclusive evidence for a phase transition in the temperature range 25 - 600 K.

1. Introduction

In his classical treatise Wells [1] remarked that it is not unambiguously possible to correlate the coordination geometry with the assumed valences of copper in its sulphides. Compounds in which the stoichiometric formula implies that copper appears with mixed valence often display physical properties which cannot be explained on that basis. However, the assumption that copper is always monovalent in its chalcogenides, except the oxides, yields a more consistent picture. This hypothesis [2] is based on the fact that the p orbital energy levels of sulphur and selenium lie close to that of iodine which forms no stable compounds with divalent copper. In the solid state the Cu d¹⁰ band is completely filled and is situated below the top of the p band of the non-metal.

This view is slowly gaining acceptance. It is possible to make a direct experimental determination of the valence state by means of X-ray photoelectron spectroscopy (XPS) (electron spectroscopy for chemical analysis). One important feature of the copper core spectrum is the presence of the so-called satellite peaks for divalent copper. Their unique assignment was demonstrated by van der Laan *et al.* [3] in his work on copper halides using a combination of XPS and Auger spectroscopy data. Advantage was taken of this feature in a number of XPS investigations of binary chalcogenides,

*Present address: Institute of Chemistry, University of Uppsala, Box 531, S-751 21 Uppsala, Sweden.

and the results obtained by Folmer and Jellinek [4] as well as others reported in the literature [5, 6] support the assumption that copper is also monovalent in ternary chalcogenides.

In compounds such as CuS and KCu_4S_3 the presence of monovalent copper demands a non-integer assignment for the chalcogen valence. According to the crystal structure determinations there are two types of sulphur atom in KCu_4S_3 [7] but there is no pair formation, whereas in CuS both singlets and pairs occur [8] corresponding to the formula $\text{Cu}_3\text{S}[\text{S}_2]$. Both compounds display metallic properties [9, 10] consistent with the assumption that the electron deficit (relative to a closed-shell configuration for the chalcogen) is delocalized. We believe that such holes in the valence band (which has a predominant chalcogen p character) may be fairly stable in the copper chalcogenides, particularly in the heavier chalcogens.

We have investigated the properties of TlCu_2Se_2 . This compound exhibits metallic conduction [11] which has been explained as being a consequence of the presence of both thallium(I) and thallium(III) atoms. We question this explanation on crystal chemical grounds as there is only one crystallographic site for each type of atom. We believe that the metallic conductivity is due to there being one hole in the valence band per formula unit. We have obtained support for this explanation from measurements of some fundamental physical properties (electrical transport, magnetic susceptibility), the results of which are presented in this paper.

2. Experimental details

2.1. Synthesis

TlCu_2Se_2 was made in two stages. Thallium (Aldrich; purity, 99.999%), which had been purified by exposure to a hydrogen stream to remove surface oxides, was reacted with selenium (Koch-Light; purity, 99.95%) in a Pyrex tube at 570 K to form TlSe . This product is much more stable towards oxidation than is commercial Tl_2Se which was used in preliminary tests. In the second step selenium and copper (Koch-Light; purity, 99.999%) were reacted with TlSe at 670 K. The product was polycrystalline, although some regularly aligned single-crystal flakes like packs of cards were obtained. A scalpel was used to extract single crystals suitable for some of the measurements.

2.2. X-ray diffraction

The products of the synthesis were monitored by X-ray powder diffraction using a Guinier-Hägg camera equipped with highly monochromatic $\text{Cu K}\alpha_1$ radiation ($\lambda = 1.540\,596\text{ \AA}$) [12, 13]. The camera was calibrated using silicon as an internal standard ($a = 5.431\,028\text{ \AA}$ at 295.6 K [12]).

A powder diffractometer ($\text{Cu K}\alpha$ radiation) equipped with a helium flow cryostat was used for the low temperature recordings, and the high temperature experiments were performed with a Guinier-Simon camera.

Silicon, which was assumed to have a linear expansion coefficient of $2.56 \times 10^{-6} \text{ K}^{-1}$ [14], was mixed with the sample in the capillary.

The cell parameters were refined using a least-squares procedure which took into account the individual errors (due to variations in the intensity or line quality) in the measurements of the Bragg angles and the non-linear transfer of these errors when refining the corresponding $\sin^2\theta$ (or Q) values [15].

2.3. Physical measurements

The electrical conductivity and Hall effect of compressed powders and single crystals were measured in the temperature range 4.2 - 300 K. Five metal contacts were painted onto copper printed on a resin plate onto which the specimen was glued. Thin copper leads were soldered onto the printed copper and the plate was fitted into a specimen holder on a long rod inside a helium cryostat.

The sample dimensions and the distance between the contacts were determined optically using a microscope equipped with a measuring device (an eyepiece with a maximum resolution of $2 \mu\text{m}$ at the highest magnification) which was calibrated against a standard millimetre scale (Olympus). The relative error in these measurements is estimated to be of the order of 5% for compressed powder but can be as great as 20% for very thin ($20 - 30 \mu\text{m}$) single crystals. The contacts were initially made using silver paint but this procedure yielded non-reproducible results, possibly because of silver migration. Platinum paint (Demetron) gave more satisfactory results although there were still problems owing to contact breaks.

The helium cryostat was equipped with a superconducting coil (Oxford Instruments) which was used to increase the amplitude of the Hall field, which oscillated about zero, up to 1 T. Separate a.c. currents with frequencies of the order of 1 Hz but with no common factor were taken from a single oscillator to the sample and the magnetic coil. The voltage signals for the conductivity and the Hall effect measurements were detected with lock-in amplifiers (Princeton Applied Research) coupled to a small computer (ITT Apple system) which was used for averaging [16]. The Hall voltage was typically of the order of 10^{-8} V .

Thermoelectric data were obtained from measurements performed on a compressed powder pellet clamped between two pieces of gold. The Seebeck coefficient at temperatures in the range 20 - 300 K was calculated as the slope of the plot of thermovoltage *versus* temperature gradient using a least-squares fitting. The temperature gradients were kept as small as possible to ensure a linear dependence. Since the Seebeck coefficient of TiCu_2Se_2 is rather small, a correction for the contribution from the gold contacts had to be made. The gold contacts were calibrated against lead, the Seebeck coefficient of which is accurately known [17].

The magnetic susceptibility between 4.2 and 300 K was measured using the Faraday method in a device equipped with a superconducting system (Oxford Instruments). The field gradient (maximum, 10 T m^{-1})

could be regulated independently of the field (maximum, 5 T). The apparatus was equipped with a Mettler ME21 electronic vacuum microbalance (null method). The data collection and the susceptibility calculations were performed using a small computer (ITT Apple system).

3. Results

3.1. X-ray diffraction

The structure of TlCu_2Se_2 (Fig. 1) was determined from electron diffraction data [18] and was later confirmed and refined from X-ray diffraction data [19]. It contains only one crystallographic site for each type of atom. Thallium has eight selenium neighbours and copper has four. The structure can be classified as the ThCr_2Si_2 type although the c/a ratio of the body-centred tetragonal cell is rather high compared with that of typical metallic structures where the non-metal atoms form pairs along the c axis in some cases. TlCu_2Se_2 can be visualized as a layer compound with metal-like bonding within the Cu-Se layers (interconnected tetrahedra) which are connected by more ionic Tl-Se bonds [19]. The bonding is reflected in the crystal habit.

We found only small differences between the cell parameters of single-phase specimens and of samples containing TlCuSe or TlCu_4Se_3 [20]. Our data are in satisfactory agreement with previous investigations (Table 1). The homogeneity range is thus likely to be restricted.

We made diffraction measurements at low and high temperatures to determine whether a phase transition occurred. The cell parameter data are

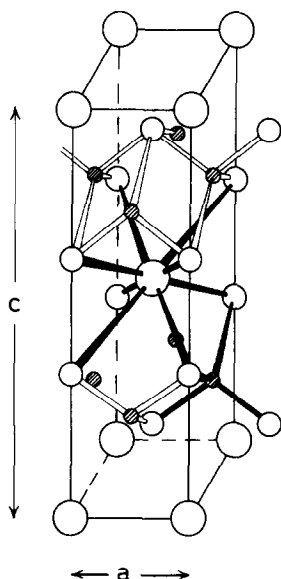


Fig. 1. The crystal structure of TlCu_2Se_2 : \bigcirc , thallium; \circ , selenium; \odot , copper.

TABLE 1

The tetragonal unit cell parameters of TiCu_2Se_2 determined in this work and reported in the literature

Cell parameter		Reference
a (Å)	c (Å)	
3.852(2)	14.01(1)	[19]
3.8522(6)	14.029(1)	[11]
3.8533(5)	14.017(3)	[4]
3.8557(3) ^a	14.034(2)	This work
3.8562(2) ^b	14.034(2)	This work
3.8572(2) ^c	14.038(1)	This work

The numbers in parentheses denote the standard deviation of the last digit.

^a TiCu_4Se_3 present.

^b TiCuSe present.

^cSingle-phase specimen.

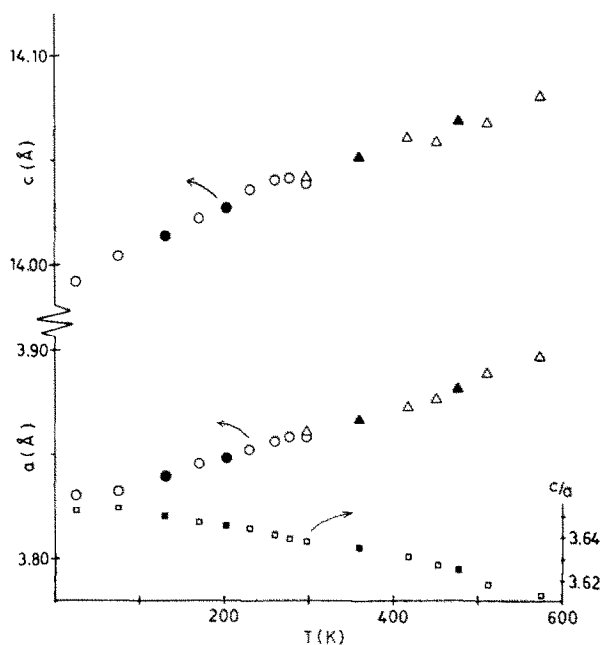


Fig. 2. The temperature dependence of the cell parameters a , c and the axial ratio c/a : \circ , diffractometer data; \triangle , film data; \bullet , \blacktriangle , data obtained on cooling.

presented graphically in Fig. 2 where it can be seen that the temperature dependence of the a axis is almost linear but the dependence of c is more complicated. However, we must strongly emphasize that the result of a least-squares refinement can be extremely sensitive to the individual weighting of the reflections, particularly those with high indices. The c axis data are

therefore less certain. We cannot exclude the possibility that our values are affected by some systematic errors since the weighting was applied on the basis of estimated measurement errors. This procedure, although crude, is better than tacitly ignoring the influence of measuring errors as is a frequent practice in handling data for a least-squares analysis [15, 21].

3.2. Resistivity measurements

Measurements of the resistivity ρ of compressed powder and single crystals yielded almost identical results within the estimated errors. The temperature dependence illustrated in Fig. 3 is typical for a metal. Our values are quite compatible with previous measurements [20].

A sample containing nickel, which was present as an impurity in the selenium used, had a rather higher resistivity than that of the compound made from selenium which had been purified by sublimation. Metallic conduction is thus likely to be characteristic of the true ternary compound.

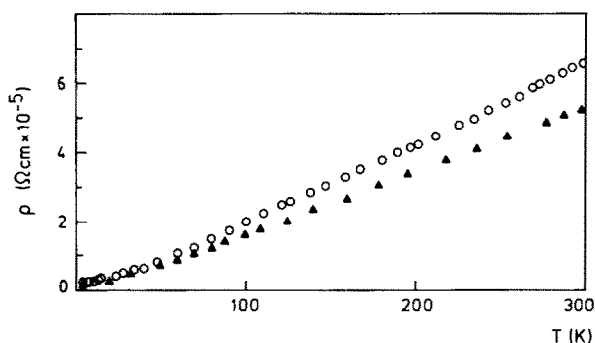


Fig. 3. The temperature dependence of the resistivity ρ : ○, compressed powder ($\rho_{300}/\rho_{4.2} \approx 24$); ▲, single crystal ($\rho_{300}/\rho_{4.2} \approx 32$).

3.3. Hall effect measurements

The magnitude and sign of the Hall coefficient give direct information about the number and type (holes or electrons) of charge carriers if only one type of carrier is present. It is extremely important to measure this effect to obtain supporting evidence for our hypothesis.

The Hall coefficient was found to be temperature independent (Fig. 4). This result shows that we are likely to encounter only one type of carrier. Therefore we can use the measured average of the Hall constant R_H ($6.4(3) \times 10^{-10} \text{ m}^3 \text{ C}^{-1}$) to calculate the hole concentration p from the formula (SI units)

$$R_H = \frac{1}{pe} \quad (1)$$

We obtain $p = 9.6 \times 10^{27} \text{ m}^{-3}$. When the cell volume measured by X-ray diffraction is used this value is equivalent to one hole per formula unit

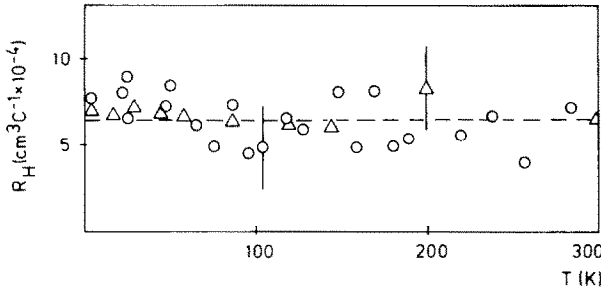


Fig. 4. The temperature dependence of the Hall constant: \circ , compressed powder; \triangle , single crystal; — — —, value expected on the basis of one hole per formula unit TiCu_2Se_2 . The vertical bars represent an error of one standard deviation.

TiCu_2Se_2 (with an error of 4%), in excellent agreement with our expectations. A similar result (0.97 hole) was obtained for the isostructural TiCu_2Te_2 [11].

By combining the resistivity and Hall effect data we can calculate the mobility of the holes from the relation $\mu_H = R_H/\rho$. μ_H had a value of $10 \text{ cm}^2 \text{ V}^{-1} \text{ s}^{-1}$ at 300 K and was approximately 30 times higher at 10 K (Fig. 3).

3.4. Thermoelectric measurements

Measurement of the Seebeck coefficient was considered to be an important complement to measurement of the Hall coefficient. The sign of the Seebeck coefficient provides confirmation of the sign of the charge carriers, and its temperature dependence gives information about the Fermi energy and the density of states at the Fermi level.

The Seebeck coefficient shows an almost linear dependence on temperature above 100 K (Fig. 5). In a broad band metal the Seebeck coefficient S is given by

$$S = \frac{\pi^2}{3} \frac{k_B}{e} \frac{k_B T}{E_F} \quad (2)$$

where E_F is the Fermi energy (a more rigorous treatment is given by Ziman [22]). When this formula was used a value of 1.3 eV was obtained for E_F from the slope of the plot of S versus T at high temperatures. This value is of the same order as that characteristic of broad band metals, and thus we can assume behaviour typical of a spherical band. Therefore we calculated the effective mass m^* from the formula [22]

$$E_F = \frac{\hbar^2}{2m^*} (3\pi^2 p)^{2/3} \quad (3)$$

using the hole concentration p from our Hall effect data. The result $m^* = 1.3m_0$ is what is expected if the top of the valence band has mainly an Se 4p character.

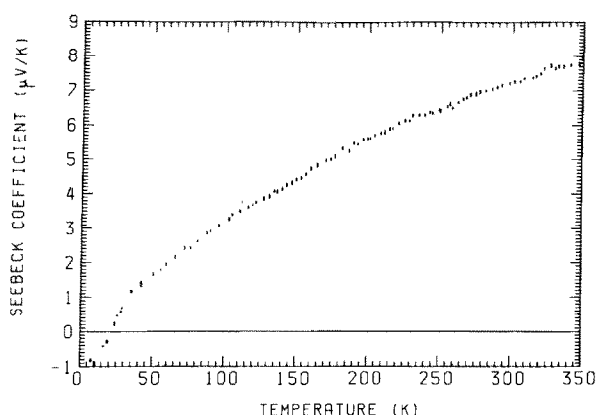


Fig. 5. The temperature dependence of the Seebeck coefficient.

3.5. Magnetic measurements

We performed magnetic measurements on a sample containing nickel (see above) in addition to the compound prepared using purified selenium. The susceptibility was almost temperature independent in both cases except for the existence of a “paramagnetic tail” at low temperatures (Fig. 6(a)). We believed that the tail was due to parasitic effects and assumed that we could divide the total susceptibility into an intrinsic component and a component which obeyed the Curie law [23]:

$$\chi_{\text{obs}} = \chi_{\text{intr}} + \frac{C}{T} \quad (4)$$

When we plotted the total susceptibility *versus* T^{-1} positive slopes roughly corresponding to the Curie constant of a (parasitic) paramagnetic contribution was obtained. The nickel-containing specimen gave $C \approx 4 \times 10^{-3} \text{ cm}^3 \text{ K mol}^{-1}$ which appears to correspond to the nickel content obtained from chemical analysis (0.2 at.% Ni per selenium atom). For the purified sample $C \approx 2 \times 10^{-4} \text{ cm}^3 \text{ K mol}^{-1}$, i.e. much less than the nickel-containing sample.

We believe that these results provide strong evidence that the paramagnetic tail is due to a contaminant. However, the method used does not allow an accurate determination of the Curie constant. In the plots shown in Fig. 6(b) the parasitic term of eqn. (4) was subtracted from the total susceptibility for the two specimens and the Curie constants were varied slightly. The curves should have become coincident, but at best we were able to make them approximately parallel for C values of $3.8 \times 10^{-3} \text{ cm}^3 \text{ K mol}^{-1}$ and $2.3 \times 10^{-4} \text{ cm}^3 \text{ K mol}^{-1}$ for the nickel-containing and pure samples respectively. The approximately temperature-independent susceptibilities became $-6 \times 10^{-6} \text{ cm}^3 \text{ mol}^{-1}$ and $-24 \times 10^{-6} \text{ cm}^3 \text{ mol}^{-1}$ respectively. Substitution of these values in eqn. (4) gave the full curves shown in Fig. 6(a). The difference of $18 \times 10^{-6} \text{ cm}^3 \text{ mol}^{-1}$ may be due to a systematic error. However, this difference is of the same order as the uncertainty in

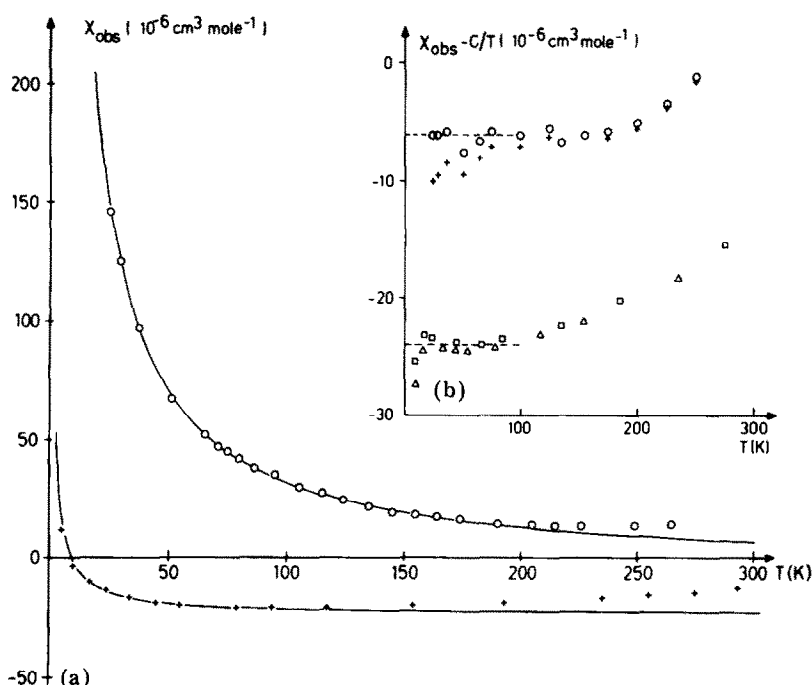


Fig. 6. (a) The measured susceptibility of two different samples of TiCu_2Se_2 ($B_0 = 0.875$ T) (\circ , specimen containing nickel; +, specimen prepared using sublimated selenium; —, calculated from eqn. (4) (see text)) and (b) the susceptibility after subtracting a paramagnetic term (the upper symbols correspond to the nickel-containing specimen of Fig. 6(a) and the lower symbols apply to the purified specimen) (\circ , $C = 3.8 \times 10^{-3} \text{ cm}^3 \text{ K mol}^{-1}$; +, $C = 3.9 \times 10^{-3} \text{ cm}^3 \text{ K mol}^{-1}$; \square , $C = 2.3 \times 10^{-4} \text{ cm}^3 \text{ K mol}^{-1}$; \triangle , $C = 2.5 \times 10^{-4} \text{ cm}^3 \text{ K mol}^{-1}$; ---, approximately temperature-independent terms (see text)).

the total diamagnetic contribution and its origin does not fundamentally alter the conclusion that TiCu_2Se_2 does not show any intrinsic Curie behaviour as would have been the case if divalent copper had been present. Rather, we find a roughly temperature-independent intrinsic contribution of approximately $100 \times 10^{-6} \text{ cm}^3 \text{ mol}^{-1}$ after correction for the diamagnetic contribution ($-120 \times 10^{-6} \text{ cm}^3 \text{ mol}^{-1}$).

For comparison, values of $(60 - 110) \times 10^{-6} \text{ cm}^3 \text{ mol}^{-1}$ have been reported [10, 24] for MCu_4S_3 ($M \equiv \text{K, Rb, Cs}$) metallic compounds with similar structural features [7, 25] which, according to Hall effect data [4], are likely to contain one hole per formula unit. The ternary copper sulphide $\text{Na}_3\text{Cu}_4\text{S}_4$, which is also metallic, has a temperature-independent susceptibility of about $150 \times 10^{-6} \text{ cm}^3 \text{ mol}^{-1}$ [24, 26].

If a single-carrier (hole) formalism and a single-valley hole pocket with $p' = 1$ hole per formula unit TiCu_2Se_2 (Hall effect data) and $E_F = 1.3$ eV (Seebeck effect data) are assumed, the free-electron Pauli susceptibility

$$\chi_P^0 = \frac{2}{3} \mathcal{N}(E_F) \mu_B^2 = \frac{p}{E_F} \mu_B^2$$

has a value of $25 \times 10^{-6} \text{ cm}^3 \text{ mol}^{-1}$. If a multivalley hole pocket with degeneracy g ($g \approx 3$ for Se 4p valence band states) is assumed, the calculated free-electron Pauli susceptibility becomes a factor of $g^{2/3} = 3^{2/3} \approx 2$ larger, *i.e.* approximately $50 \times 10^{-6} \text{ cm}^3 \text{ mol}^{-1}$.

The value estimated from the observed molar susceptibility is roughly twice the calculated value. Although some enhancement may be possible owing to correlations of the holes at the top of the Se 4p valence band where the validity of the one-electron approximation (see above) is doubtful, a lower value of χ_p is obtained if we assume that the intrinsic susceptibility also contains a contribution from Van Vleck band paramagnetism. For large covalency and small excitation energies such a contribution could be of the order of $50 \times 10^{-6} \text{ cm}^3 \text{ mol}^{-1}$. The observed magnetic susceptibility after subtraction of the Curie-like tail due to the presence of some paramagnetic $\text{Ni}^{2+} \text{ d}^8$ ions increases slightly with increasing temperature (Fig. 6(b)) which may indicate the importance of Van Vleck contributions to the intrinsic susceptibility of TlCu_2Se_2 .

In conclusion, the observed susceptibility (Fig. 6(a)) may be composed of a parasitic Curie-like contribution and contributions from diamagnetism and Pauli and Van Vleck band paramagnetism due to the threefold valley character of the spin-orbit-coupled Se 4p hole states.

4. Conclusions

The results of the physical measurements are all in good agreement with the initial hypothesis that copper is monovalent in TlCu_2Se_2 . Hall and Seebeck effect data indicate that the metallic properties and the low temperature-independent paramagnetism are due to valence band holes. The holes have a broad band character (relatively high mobility and low effective mass) consistent with the assumption that they are situated at the top of the valence band. This has a predominant Se 4p character, and we can formally express the valence situation as corresponding to $\text{Tl}^+\text{Cu}_2^+\text{Se}_2^{-3/2}$. Although valence band holes are energetically unstable with regard to the electron energy, we found no conclusive evidence from X-ray powder diffraction data obtained over a wide temperature range (25 - 600 K) that the compound undergoes a phase transition.

We shall report on the quaternary system $\text{TlCu}_{2-x}\text{Fe}_x\text{Se}_2$ in a forthcoming paper.

Acknowledgments

The authors wish to thank Mrs. R. J. Haange and Mr. H. C. G. Druiven for their assistance with the electrical transport and magnetic susceptibility measurements.

This investigation was supported by The Netherlands Foundation for Chemical Research with financial aid from The Netherlands Organization for the Advancement of Pure Research which is gratefully acknowledged.

References

- 1 A. F. Wells, *Structural Inorganic Chemistry*, Oxford University Press, London, 1962.
- 2 F. Jellinek, *MTP International Review of Science, Inorganic Chemistry Series 1*, Vol. 5, Butterworths, London, 1972, p. 339.
- 3 G. van der Laan, C. Westra, C. Haas and G. A. Sawatzky, *Phys. Rev. B*, **23** (1981) 4369.
- 4 J. C. W. Folmer and F. Jellinek, *J. Less-Common Met.*, **76** (1980) 153.
- 5 H. Rupp and U. Weser, *Bioinorg. Chem.*, **6** (1976) 45.
- 6 I. Nakai, Y. Sugitani, K. Nagashima and Y. Niwa, *J. Inorg. Nucl. Chem.*, **40** (1978) 789.
- 7 W. Rüdorff, H. G. Schwarz and M. Walter, *Z. Anorg. Allg. Chem.*, **269** (1952) 141.
- 8 L. G. Berry, *Am. Mineral.*, **39** (1954) 504.
- 9 F. Jellinek, in G. Nickless (ed.), *Inorganic Sulphur Chemistry*, Elsevier, Amsterdam, 1969.
- 10 D. B. Brown, J. A. Zubieta, P. A. Vella, J. T. Wroblewski, T. Watt, W. E. Hatfield and P. Day, *Inorg. Chem.*, **19** (1980) 1945.
- 11 G. Brun, B. Gardes, J.-C. Tédénac, A. Raymond and M. Maurin, *Mater. Res. Bull.*, **14** (1979) 743.
- 12 M. Hart, *J. Cryst. Growth*, **55** (1981) 409, and references cited therein.
- 13 M. Deutsch and M. Hart, *Phys. Rev. B*, **26** (1982) 5558.
- 14 R. D. Deslattes, A. Henins, H. A. Bowman, R. M. Schoonover, C. L. Carroll, I. L. Barnes, L. A. Machlan, L. J. Moore and W. R. Shields, *Phys. Rev. Lett.*, **33** (1974) 463.
- 15 A. G. Worthing and J. Geffner, *Treatment of Experimental Data*, Wiley, New York, 1940.
- 16 H. C. G. Druiven, *Materials Science Centre Rep.*, 1980, p. 74 (University of Groningen).
- 17 F. J. Blatt, P. A. Schroeder, C. L. Foiles and D. Greig, *Thermoelectric Power of Metals*, Plenum, New York, 1976.
- 18 A. S. Avilov, R. M. Imamov and Z. G. Pinsker, *Sov. Phys. — Crystallogr.*, **16** (1971) 542.
- 19 K. Klepp and H. Boller, *Monatsh. Chem.*, **109** (1978) 1049.
- 20 J.-C. Tédénac, G. Brun and M. Maurin, *Rev. Chim. Minér.*, **18** (1981) 69.
- 21 J. Mandel, *The Statistical Analysis of Experimental Data*, Wiley-Interscience, New York, 1964.
- 22 J. M. Ziman, *Electrons and Phonons*, Oxford University Press, Oxford, 1960; *Principles of the Theory of Solids*, Cambridge University Press, Cambridge, 2nd edn., 1972.
- 23 R. Saez Puche, M. Norton and W. S. Glaunsinger, *Mater. Res. Bull.*, **17** (1982) 1429.
- 24 B. P. Ghosh, M. Chaudhury and K. Nag, *J. Solid State Chem.*, **47** (1983) 307.
- 25 K. Klepp, H. Boller and H. Völlenkle, *Monatsh. Chem.*, **111** (1980) 727.
- 26 Z. Peplinski, D. B. Brown, T. Watt, W. E. Hatfield and P. Day, *Inorg. Chem.*, **21** (1982) 1752.